

Performance of plastic wastes in fiber-reinforced concrete beams

F.S. Khalid^{a,*}, J.M. Irwan^a, M.H. Wan Ibrahim^a, N. Othman^b, S. Shahidan^a

^aJamilus Research Center (JRC), Faculty of Civil and Environmental Engineering, Universiti Tun Hussein Onn Malaysia, Parit Raja 86400, Johor, Malaysia

^bMicropollutant Research Centre (MPRC), Faculty of Civil and Environmental Engineering, Universiti Tun Hussein Onn Malaysia, Parit Raja 86400, Johor, Malaysia



HIGHLIGHTS

- Synthetic fibers did not affect the control behavior of beam at the yield and ultimate loads.
- At the cracking stage of beam containing fibers showed that the strength of the first crack improved compared to the normal concrete.
- The synthetic fibers in the reinforced concrete produced significant results, particularly in the linear elastic region.
- The mechanism fiber bridging of the RPET fiber was more evident compared to the irregularly shaped fibers.
- The RPET fibers incorporated into the concrete failed by rupture, which is caused by the tensile stress.

ARTICLE INFO

Article history:

Received 5 February 2018

Received in revised form 10 June 2018

Accepted 14 June 2018

Keywords:

Waste plastic

Synthetic fiber

Fiber concrete

Beam reinforced concrete

ABSTRACT

Synthetic plastics are typically discarded, thus causing environmental pollution. Plastic wastes are recycled as fiber in concrete to solve this problem. In this study, synthetic fibers in a concrete matrix were investigated through compressive strength, splitting tensile, fracture energy, and flexural beam tests. The results show that an increase in fiber content improves the tensile strength of the concrete matrix. A high fiber content results in a substantial amount of fibers crossing a fractured section, thereby activating failure resistance mechanisms. Ring-shaped fibers, which are mainly designed to activate fiber yielding instead of fiber pullout, are better than irregularly shaped polyethylene terephthalate and waste wire fibers. Incorporating plastic fibers into concrete does not significantly change the failure mode of reinforced concrete beams compared to that of normal concrete beams. However, the first crack load presented improved results. The reinforced concrete containing ring-shaped plastic fibers with a width of 10 mm (RPET-10) exhibited remarkable results during the first crack load with an increment of 32.3%. It can be concluded that ring-shaped PET waste produces fiber concrete with a performance comparable to that of commercial synthetic fibers.

© 2018 Elsevier Ltd. All rights reserved.

1. Introduction

The amount of synthetic plastic consumed annually has been steadily increasing. The intensifying synthetic plastic consumption can be ascribed to the practical features of synthetic plastic, namely, factory fabrication, lightness of plastic products and low production cost [1,2]. Plastic has been extensively used in bottles and food casings, industrial products, communication materials and housing, among other uses. Although several methods have been employed for the disposal of synthetic wastes, most treatments are inadequate because of excessive synthetic waste generation. Therefore, one of the alternatives is to recycle synthetic wastes and use them as fiber reinforcement for concrete. Synthetic

fibers are popular for reinforcing lightweight precast concrete elements such as double walls, pipes and sleepers [3,4,5]. These applications can effectively control cracks [6] and prevent dry shrinkage cracks of concrete [7]. Besides, synthetic fibers have been used to improve the toughness of concrete with enhanced crack resistance [8]. Foti [9] studied the use of polyethylene terephthalate (PET) bottles as fiber to improve concrete ductility and found that the average tensile strength of the ring-shaped fibers is sufficiently high and comparable to the most commonly used carbon or steel fiber to reinforce concrete. The PP/PE blended fiber reinforced composites (HyFRCs) at fiber volume as 2.9% obtained mechanical enhancement of $38 \pm 2\%$ on compressive and $40 \pm 1\%$ flexural strengths compared to normal concrete [10]. Morphological observations show strong mechanical interactions between fibers and the cement matrix as similar to the chemical/mechanical interactions observed for polyacrylonitrile reinforced composites

* Corresponding author.

E-mail address: faisalsh@uthm.edu.my (F.S. Khalid).

(PANFRCs). A comparison between steel fiber and synthetic fiber has been made. It shows that all types of fibers in concrete seem to yield better results for the same fiber content. In addition, the improvement appears to decrease when the total fiber content increases above a volume fraction of 1% [11]. The high fiber content can cause difficulty in mixing, which leads to poor compaction, non-uniform distribution of fibers, and an increase in void volume [11,12]. Foti [13] studied mechanical behavior of 3 types of possible structural reinforcing with rheoplastic mortar on reinforced concrete pillars. Foti [13] claimed that whole reinforcement (30 cm) of the concrete core obtains significant result compared to specimen with rheoplastic mortar covered at height of 28 cm.

Many researchers claimed that the pullout fiber strength increases as the embedded length of the fibers increases in the concrete matrix [14,15]. The embedded length range of 45–55 mm increased the fiber strength by 39.3%–48.1% according to Richardson et al. [16]. This difference is related to the surface fiber area connected to surface concrete as this area determines the friction of the fiber and interfacial bond energy [17,18]. In their study, Ochi et al. [19] found that polyvinyl alcohol (PVA) fibers exhibited the highest tensile strength, whereas PET fibers had the lowest tensile strength (172 MPa) [19]. The smooth surface of fibers such as polypropylene (PP) fibers has a weak bond with concrete thereby preventing sufficient friction between concrete and fibers [20]. Compared to commercial plastic fibers, PET fibers exhibit adequate tensile strength. The surface contact area between the fibers and concrete influences both pullout energy and interfacial energy [6,17]. A high pullout energy is produced by a high area of surface fiber that is connected to the concrete. Fibers measuring 15, 20, and 24 mm in length with 0.4% of PP fiber content were used in a study by Vairagade et al. [21]. The authors found that the average strength values ranged from 1.2% to 4.5% for fibers measuring between 15 mm and 24 mm in length. A long fiber has a large surface area that is connected to the concrete matrix. It can be concluded that interfacial bond strength and friction energy during load compression are higher than those of a short fiber. Therefore, fiber surface area which depends on fiber length significantly influences strength.

The increase in PET fiber content also increases tensile strength. Irwan et al. [22] observed there was increased strength for concrete with 0.5% of fiber content compared to normal concrete. Irwan et al. [22] claimed that fiber content is not the main component that improves the compressive strength of Fiber Reinforced Concrete (FRC). Instead, it is the shape and size of the fibers which influence compressive strength [23]. Ramadevi et al. [24] found that concrete containing 2% of waste PET as fine aggregate material exhibited an increase in compressive strength compared to normal concrete. The concrete containing 0.5% and 1% of fiber content demonstrated an increase in strength of 4.0% and 15% respectively compared to normal concrete. In fact, most of the researchers said that the PP and high-density polyethylene (HDPE) fibers have high resistance towards an alkaline environment, which is no agreement about the durability of PET fibers in a concrete matrix [25,26]. In addition, the SEM picture of the polymer mortar matrix shows that it has very low porosity in comparison to the cement mortar of even various grade [27]. Nili et al. [28] observed an increase of 3% in the compressive strength of concrete with 0.2% fiber content. When fibers were added into concrete, the failure pattern changed from a single large crack to a group of narrow cracks [12]. The crack can be substituted by micro-cracks due to the presence of fibers bridging in concrete [28].

A long fiber indicates a high surface contact area which is able to function as fiber bridges during compression as observed by Nia et al. [29]. Therefore, a long fiber presents high friction energy against pullout stress because of the fiber-bridging mechanism. In addition, Mohammadi et al. [30] compared toughness indices

which show that mixes with long fibers have higher indice values than those with short fibers. However, it has also been observed that a concrete mix with better workability was obtained when the percentage of shorter fibers used in the mix increased. Foti [9] used waste plastic bottles as recycled fiber material. Concrete with 0.75% of ring fibers showed an increased strength of 5% compared to concrete containing 0.5% of ring fibers [9]. Foti [31] claimed that the presence of PET strips has successfully given the concrete slabs a very ductile behavior which allowed them to avoid complete failure. This confirms the improvement in impact strength and suggests various possible uses for PET reinforced concrete. Recycled PET fibers in concrete measuring 10 mm, 15 mm, and 20 mm in length with 0.18% and 0.3% of fiber content were studied by Pelisser et al. [32]. The authors found that the size of the fiber area significantly contributes to flexural toughness indices. Adding recycled PET fibers enhanced the toughness and energy absorption of FRC under flexural load. An increase in fiber length increases the size of the fiber area that is connected to the cement matrix and contributes positively to the flexural toughness indices, particularly in I_{10} and I_{20} [33,34]. Irwan et al. [22] used fiber contents of 0.5%, 1%, and 1.5% in concrete mixes to demonstrate the change in flexural toughness with fiber content; compared to 0.5% and 1% of fiber content, 1.5% of fiber content increased the flexural toughness index of I_{20} of FRC by 22.4% and 5.7%, respectively [35].

Three fiber content percentages (0.33%, 0.42%, and 0.51%) were used in Hasan et al.'s [36] study. Gradual improvements of approximately 6.48% and 6.89% were also achieved for concrete with 0.42% and 0.51% of fiber content, respectively. In plastic fiber reinforced concrete beams, Kim et al. [37] examined the deflection behavior of a reinforced concrete (beam when PET fibers were added. In this research, the specimens with manufactured synthetic fibers clearly demonstrated an improvement in deflection behavior. For reinforced concrete beams with 0.5%–1% of PET fiber content, deflection and ultimate load capacity increased by 7–8 times for deflection and 25.5%–31.9% for ultimate load capacity. Foti [38] studied beam with reinforcement bar made with PET and CFRP are arranged as continuous bars and strips, respectively. The specimen reinforced with CFRP showed a more ductile behavior compared to PET bar. However, PET bar can be used in all those cases where the operational loads are low. Currently no published data was found on the use of ring-shaped, irregular or wire wastes for fiber reinforced concrete beams. Therefore, this study aims to investigate the behavior of reinforced concrete beams containing synthetic waste, also known as fiber concrete. Compressive and fracture tests were also conducted to determine the mechanical behavior of synthetic plastic waste in concrete.

2. Materials and methods

Waste PET bottles (Fig. 1) were used in this study. The fibers used in the experiment were ring-shaped PET (RPET-5 and RPET-10) fibers with widths or cross-sectional diameters of 60 ± 5 mm, as shown in Fig. 2. The experiment also used irregularly shaped PET fibers, synthetic waste wire fibers, and manufactured synthetic macro-fibers (Mega Mesh 55), as shown in Figs. 3, 4, and 5, respectively. The sizes of the sieved waste PET granules were approximately 5–20 mm. The waste wire was cut into 55 mm lengths. The manufactured synthetic fiber used was 55 mm in length, with a tensile strength of 425 N/mm² and an aspect ratio (L_f/d_f) of 45.

The water–binder ratio was 0.55. A total of 57 specimens were prepared for the tensile strength test. All the concrete specimens were tested using three cylinders for each batch of concrete mixture. The second experiment consisted of compressive tests and tensile tests. The next experiment was a fracture energy test of



Fig. 1. Ring-shaped PET fibers.

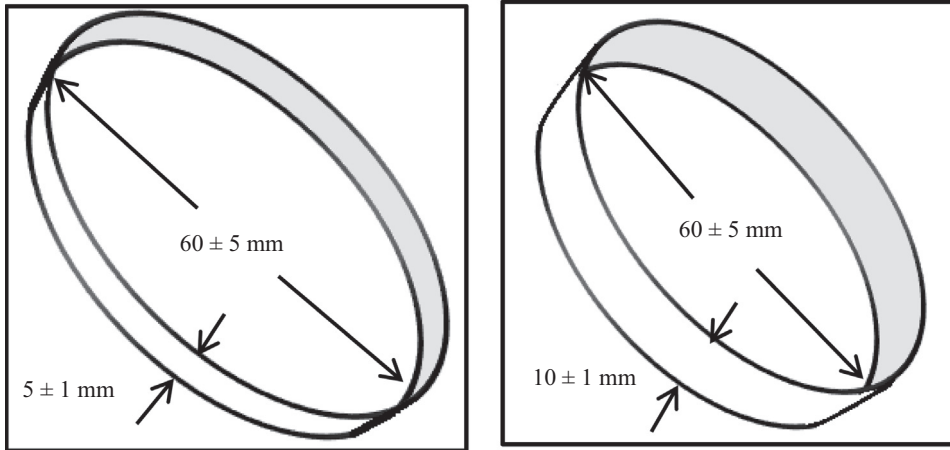


Fig. 2. The dimensions of ring-shape RPET-5 (left) and RPET-10(right).



Fig. 3. Irregularly shaped PET.



Fig. 4. Synthetic waste wire.

all concrete specimens which was conducted according to RILEM TC50-FMC. Fracture energy was determined by using 450 mm × 100 mm × 100 mm beams with an effective span beam of 400 mm and a notch depth of 25 mm as shown in Fig. 6. Three-point bending tests were conducted using a closed-loop servo electro-controlled testing machine and the load was applied at a rate of 0.4 mm/min. Fracture energy, G_F was obtained using Eq. (1).

$$G_F = \frac{W_0 + 2P_0U_0}{b(d - a_0)} \tag{1}$$

where w_0 is the area under the load deflection curve, u_0 is the maximum measured deflection, P_0 is the point-load, equivalent to the weight of the specimen, b is the specimen's thickness, d is the specimen depth and a_0 is the notch depth.

The 18 beam specimens contained ring-shaped PET (RPET-5 and RPET-10), irregular PET, wire waste and manufactured synthetic



Fig. 5. Manufactured synthetic macro-fibers.

fibers. A notch that was 4 mm wide and 33 mm deep was made at the mid-span of the beam specimen. Lastly, this experiment focused on the influence of incorporating ring-shaped PET (RPET-5 and RPET-10), irregular PET, wire waste and manufactured synthetic fibers on the flexural behavior of rectangular beams. The concrete beam was reinforced with a steel bar measuring 12 mm in diameter. The dimensions of the beams were 150 mm × 300 mm × 2500 mm. The support span was 2300 mm, and the beam was supported along the short edges as shown in Fig. 7. The 18 beam specimens were subjected to four-point loading to determine how the applied load influences the bending moment, cracking patterns, and deflection behavior of fiber concrete (FC) beams.

Vertical displacements were recorded at different points of the beams by displacement sensors. The central (maximum) displacements were measured by LVDT. Beam deflections were measured at three different points. One point was located at the middle of the span and two points were positioned at one-quarter of the span, which resulted in an equal distance of 766 mm from the support and the midpoint.

The aim of non-linear analysis in this study was to compare the behavior and pattern of beams with and without fiber concrete with those obtained from the experimental work. The non-linear finite element software that was used in this study was ATENA [39].

3. Results and discussion

This section describes the results of the compressive strength, splitting tensile strength, fracture energy and flexural beam tests. A detailed analysis was performed to study the effects of fiber content and fiber size on the performance of fibers in the concrete matrix.

3.1. Compressive and splitting tensile strength

The experimental results for compressive strength are tabulated in Table 1. This study shows that instability occurred to the compressive strength of concrete when fibers were added. Therefore, the addition of fibers in concrete does not improve the compressive strength of concrete, which is consistent with the reports by Ochi et al. [19], Oliveira et al. [23], Hsie et al. [40], Campione [41], Fraternali et al. [42] and Irwan et al. [43]. Furthermore, in this study, the increment in the compressive strength of FRC was not influenced by the volume of the added fibers.

The tensile strength of a normal specimen is 3.08 MPa, which is lower than those containing RPET-5, RPET-10, manufactured synthetic fiber, and waste wire fibers, except for the irregularly shaped PET fibers. Concrete containing ring-shaped PET fibers go through a gradual increase in tensile strength with an increase in fiber content. This has been consistently reported by Hassan et al. [36], Hsie et al. [40], Peyvandi et al. [44], Sammer et al. [45] and Southos et al. [46]. Fig. 8 shows the experimental results of the splitting tensile strength of concrete.

The experimental results indicate that RPET-5 FRC presented an increase in tensile strength of 16.9%, 26.3%, and 13.3% with 0.5%, 1%, and 1.5% of fiber content, respectively. Therefore, the strength increments ranged from 11.4% to 26.3% with fiber content ranging from 0.25% to 1.0%. Relative to the tensile strength of the normal specimen, the tensile strength values of RPET-10 FRC increased by 16.9%, 35.1%, and 24.4% for concrete with 0.5%, 1%, and 1.5% of fiber content, respectively. A gradual decrease totaling 7.4% occurred when irregularly shaped PET fibers were incorporated into concrete. This result indicates that irregularly shaped PET fibers do not improve the tensile strength of concrete to withstand the applied load. By contrast, the tensile strength of the manufactured synthetic fibers increased with increasing fiber content. The stability of the tensile strength with the addition of manufactured synthetic fibers explains the premise on FRC of Kim [37] where the addition of synthetic fibers in concrete can improve the tensile strength of concrete.

The experimental results confirmed that 1% of fiber content is the optimal value for RPET-5 and waste wire fibers, whereas

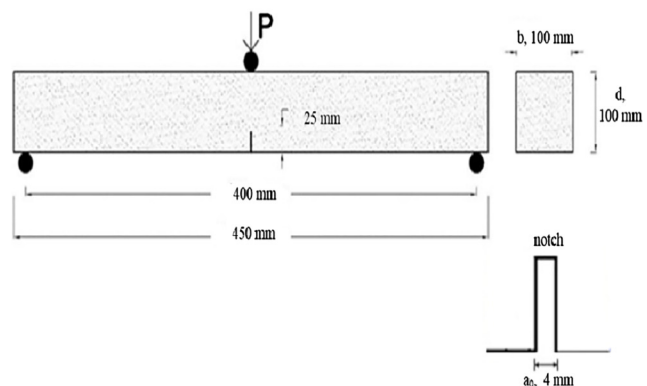


Fig. 6. Three-point loading for the fracture energy test.

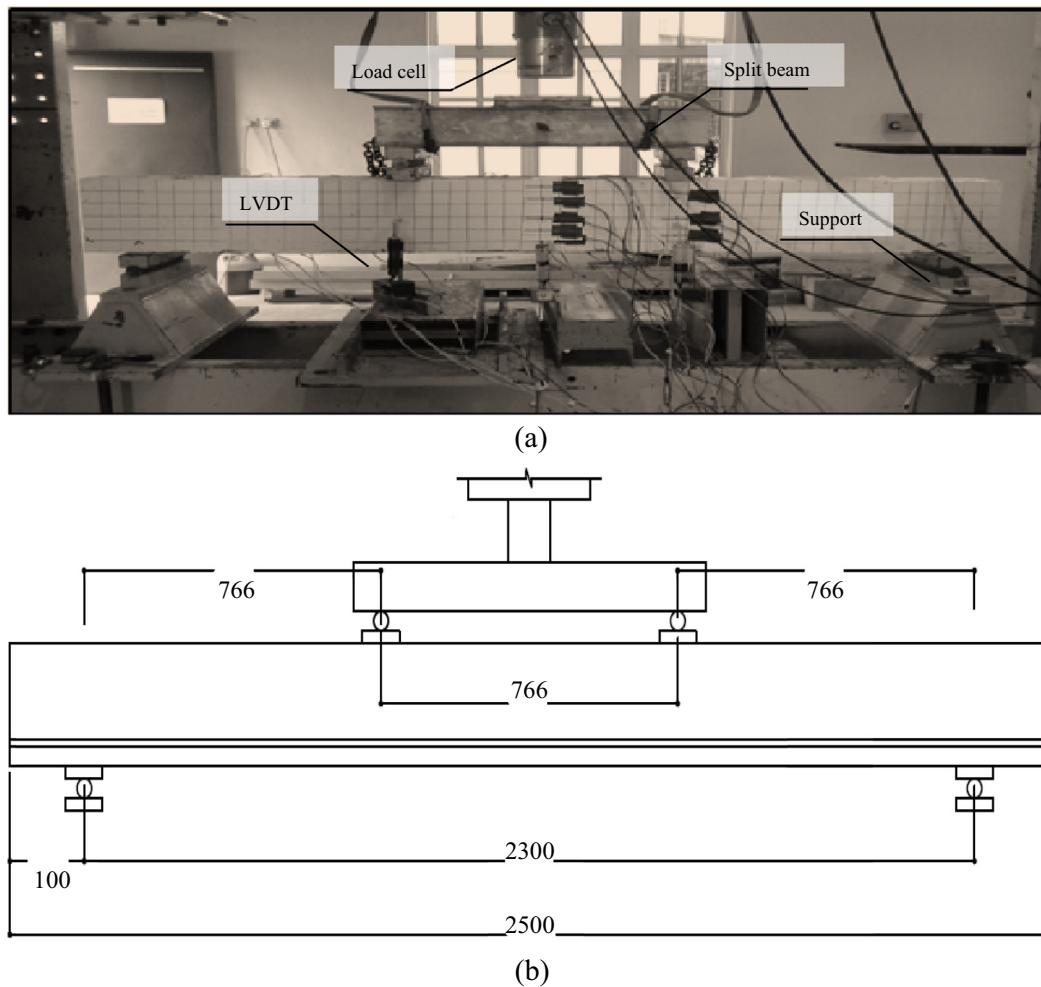


Fig. 7. (a): Beam specimen (in mm) prior to testing and (b): Loading device and support details.

Table 1
Compressive strength results.

Fiber Content (%)	Average Compressive Strength of Concrete Fiber				
	RPET-5	RPET-10	Irregular PET	Manufactured Synthetic	Wire waste
0.0	34.01 ± 0.86	34.01 ± 0.86	34.01 ± 0.86	34.01 ± 0.86	34.01 ± 0.86
0.25	34.45 ± 0.83	35.45 ± 0.99	34.10 ± 0.62	33.92 ± 1.03	34.20 ± 0.84
0.5	34.96 ± 0.32	34.96 ± 0.81	34.89 ± 0.78	34.21 ± 0.89	34.52 ± 0.51
0.75	35.29 ± 0.88	34.29 ± 0.42	33.99 ± 0.91	35.30 ± 0.44	34.37 ± 0.71
1.0	34.51 ± 0.95	34.51 ± 0.42	35.10 ± 0.52	35.01 ± 1.15	34.21 ± 1.05
1.25	34.82 ± 1.11	34.82 ± 0.92	34.73 ± 0.92	34.88 ± 0.90	34.77 ± 0.92
1.5	35.23 ± 0.80	34.23 ± 0.81	34.33 ± 0.72	34.82 ± 0.33	34.91 ± 1.01

1.25% of fiber content is the optimum fiber content for RPET-10 fiber. The manufactured synthetic fibers showed a significant increase in tensile strength up to 1.50% of fiber content. Therefore, the amount of fibers incorporated into concrete is a main factor in the tensile strength of FRC. Thus, a substantial amount of fibers incorporated into concrete can achieve the absolute maximum load (fiber yielding) and function as a fiber bridge as the load compression increases. This mechanism can be ascribed to the interlocking tensile strength of the fibers and failure up to the maximum fiber tensile strength, which may lead to slipping as the tensile load increases. Irregularly shaped PET fibers showed insignificant changes in tensile strength compared to the normal specimen. In this study, the tensile strength of concrete with

irregularly PET fibers is not influenced by the volume of the added fibers.

The post-peak failure behavior, which included the fracturing sound of fiber, was attributed to the gradual rupture of fibers. The majority of the fibers incorporated into the concrete failed by rupture, which is caused by the tensile stress subjected to the tensile load. The function of the ring-shaped PET fibers is to retain the tensile stress at the critical fiber-bridging cross section. The fiber-bridging stress until the yield point of the fiber ultimate tensile strength is reached. Thus, the load continuously ruptures the individual fibers at the fiber-bridging zone in the FRC. Fig. 9 shows the fiber reinforced concrete after being subjected to the splitting tensile stress test.

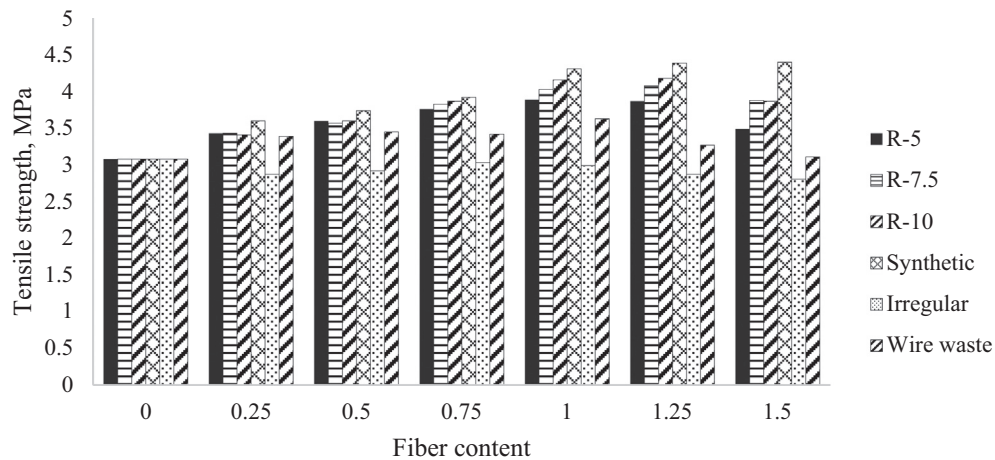


Fig. 8. Effect of fiber content on the experimental results of the splitting tensile strength of concrete.



(a). Irregular PET fiber concrete



(b). Ring shaped PET fiber concrete



(c). Wire waste fiber concrete



(d). Manufactured synthetic fiber concrete

Fig. 9. Fiber reinforced concrete after the splitting tensile strength test.

The fiber bridging mechanism of the ring-shaped PET fibers in FRC was more evident compared to that of irregularly shaped PET fibers. Compared to the irregularly shaped PET fibers, the ring-shaped PET fibers provided individual maximum tensile strength by yielding until the fiber ruptures. Meanwhile, the mechanism of the ring-shaped PET fibers is likewise different from that of the manufactured synthetic fibers which depend on interfacial bond strength. At the end of the test, it was shown that straight wire fibers easily slip and fail to resist tensile stress in the concrete matrix.

In conclusion, adding fibers, except for irregular PET fibers, improves the tensile strength of concrete. According to the tensile strength test, fiber content between 1% and 1.25% was an acceptable working range for FRC reinforced with ring-shaped PET, manufactured synthetic fiber, and waste wire fibers.

3.2. Fracture energy

The results show that concrete with fiber has the ability to better enhance fracture energy than normal concrete, as shown in Table 2. At the end of the experiment, most FC specimens achieved significant fracture energy results compared to normal concrete. All the results on the fracture energy of normal concrete and FC were obtained through the finite element method (FEM) analysis.

3.3. Mode of failure and ultimate load

This experiment was designed to fail in the flexural mode and during the crushing of concrete. During the test, the aforementioned modes were observed in all reinforced concrete beam

Table 2
Fracture energy of fiber concrete.

Beam Designation	Fracture energy, (N/m)	Difference percentage compared to normal concrete, (%)	Difference percentage compared to irregular PET FC, (%)	Difference percentage compared to synthetic FC, (%)
B-Normal	155.41 ± 3.24	–	–20.7	–49.7
B-RPET-5	228.91 ± 4.17	47.0	16.8	–26.0
B-RPET-10	231.42 ± 4.67	48.9	18.1	–25.2
B-IRE PET	196.01 ± 5.12	26.1	–	–36.6
B-SYNT	309.21 ± 3.90	99.0	57.8	–
B-WIRE	227.14 ± 2.90	46.2	15.9	–26.5

specimens. Figs. 10–15 show the typical flexural failure obtained during the tests.

As expected, the flexural failure mode of all reinforced concrete beam specimens occurred at the central zone between two-point loadings because that zone was under pure bending. The failure mode was determined when the load suddenly dropped during the test. The flexural failure mode of all tested reinforced concrete beams started after the primary crack appeared at the central zone when the distance between cracks prevented sufficient tensile stresses to develop, thereby causing further cracking. Then, the crack started opening fast and wide, thereby confirming that the flexural failure mode occurred at that crack. On average, normal reinforced concrete beams and reinforced FC beams containing irregularly shaped PET, waste wire, and synthetic fibers, showed that specimens ultimately failed through yielding of tensile reinforcement and concrete compression, as shown in Figs. 10–15. Therefore, synthetic fibers, all sizes of RPET fibers, irregularly shaped PET fibers, waste wire fibers, and manufactured synthetic fibers clearly exhibited similar failure modes. Thus, concrete would fail because of compression regardless of whether fiber has been incorporated into it or not. This confirmed that reinforced concrete beams with or without fiber were unaffected by the ultimate load,

except for synthetic straight fiber. Moreover, the results of the ultimate load of normal reinforced concrete beams and reinforced FC beams are similar in pattern in terms of strength and failure mode behavior.

The results for serviceability and ultimate loads are presented in Table 3. During the flexural test for reinforced concrete beams, the recorded serviceability load observations showed that the first crack appeared at the mid-span of the beam. The load value applied to the beam was recorded as a serviceability load the moment the first crack appeared. The value of the first crack load was estimated by examining the graphs. Once this load was achieved, the beam started to behave nonlinearly. The first crack load was determined from the load–deflection graph as shown in Figs. 16–21. The deflection of reinforced concrete beams was recorded by LVDT during the flexural beam test. This deflection was comparable with the simulation conducted using the ATENA Software.

Table 4 presents a summary of the experimental results for serviceability and ultimate loads. The experiment on normal reinforced concrete beams, namely, B-NOR-1, B-NOR-2, and B-NOR-3, showed that the first crack appeared at 17.5 kN, 17 kN, and 18.5 kN, respectively. The normal reinforced concrete beams achieved

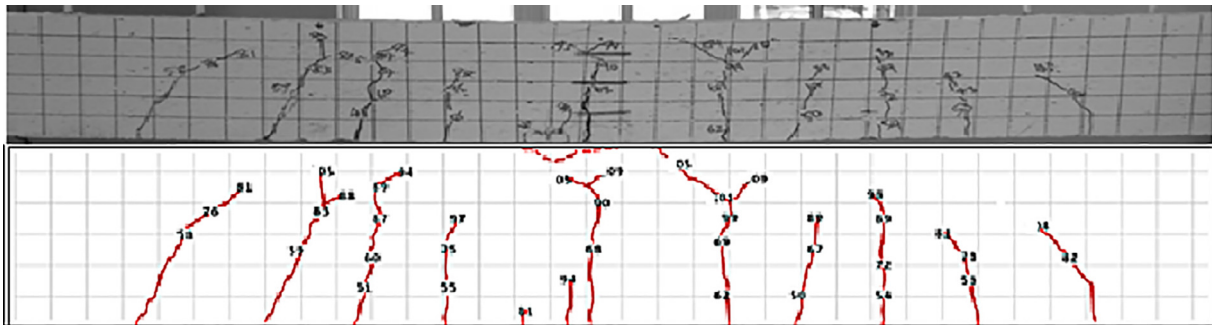


Fig. 10. Flexural failure and concrete compression for B-Normal specimen.

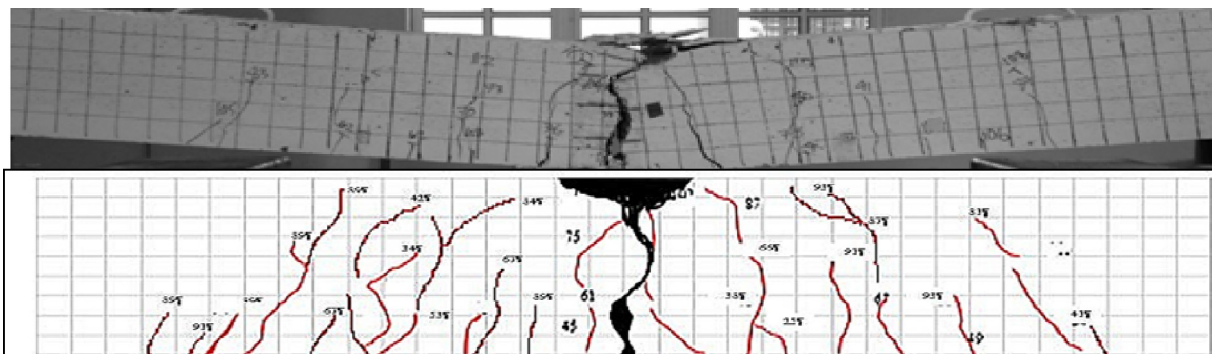


Fig. 11. Flexural failure and concrete compression for B-RPET-5 specimen.

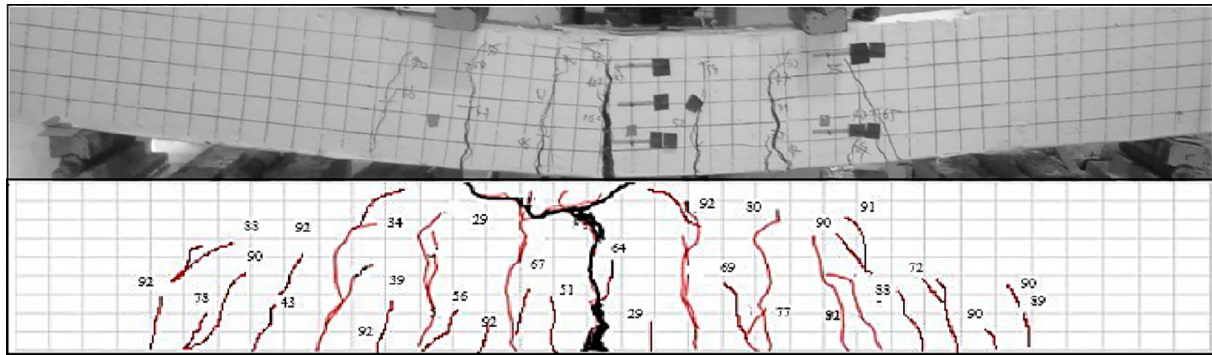


Fig. 12. Flexural failure and concrete compression for B-RPET-10 specimen.

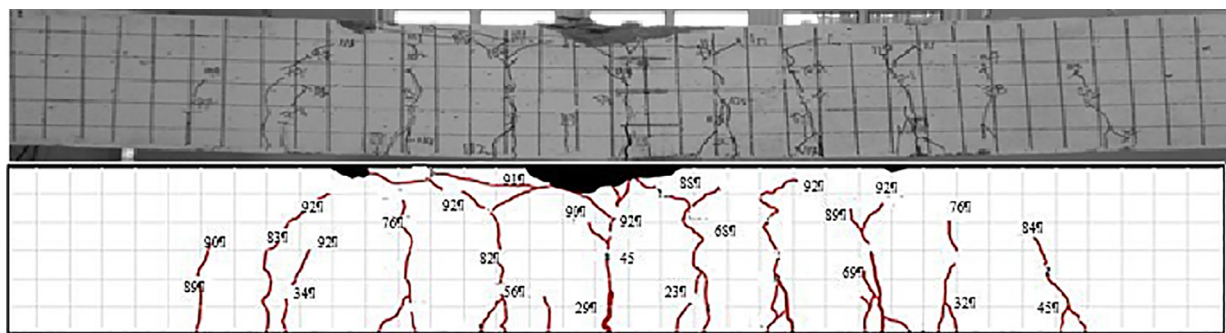


Fig. 13. Flexural failure and concrete compression for B-Irregular PET specimen.

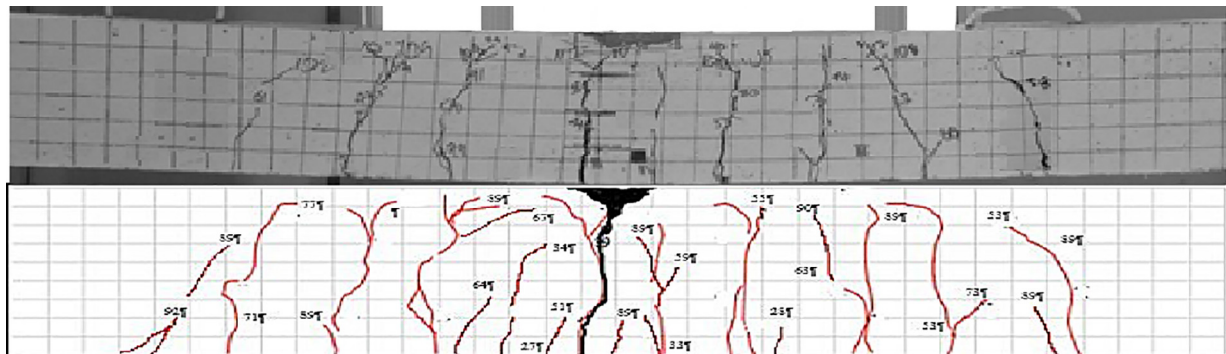


Fig. 14. Flexural failure and concrete compression for B-Wire specimen.

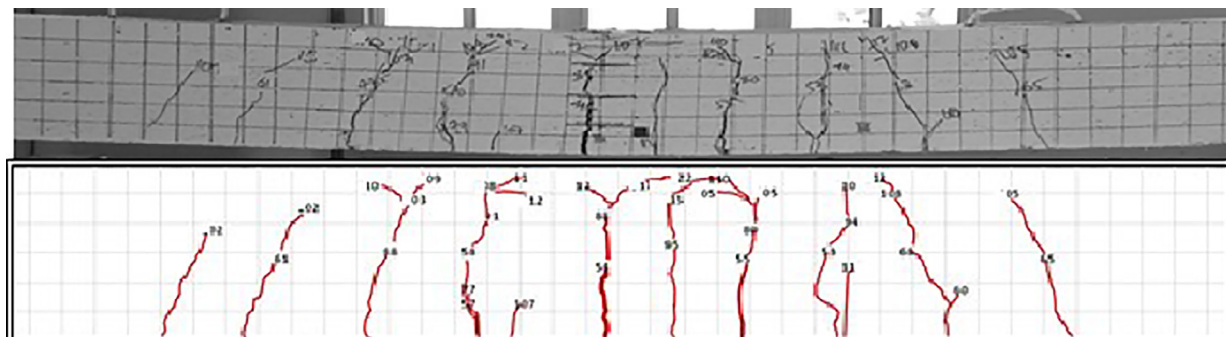


Fig. 15. Flexural failure and concrete compression for B-Synthetic specimen.

Table 3
Experimental results of serviceability load, ultimate load, and mode of failure.

No of batch	Beam Designation	Serviceability load, (kN)		Ultimate load, (kN)	Mode of failure ^a
		Observation during test	The curve of load-deflection graph		
1	B-NOR-1	26.5	17.5	99.0	A & B
	B-NOR-2	23.5	17.0	98.0	A & B
	B-NOR-3	23.5	18.5	98.5	A & B
2	B-RPET-5-1	32.5	22.0	101.0	A & B
	B-RPET-5-2	35.5	23.0	98.5	A & B
	B-RPET-5-3	36.0	23.5	102.5	A & B
4	B-RPET-10-1	34.5	24.0	99.0	A & B
	B-RPET-10-2	35.5	23.5	98.5	A & B
	B-RPET-10-3	38.0	23.0	101.5	A & B
5	B-IRE-1	30.0	22.5	99.5	A & B
	B-IRE-2	30.5	20.5	99.0	A & B
	B-IRE-3	33.5	21.5	99.5	A & B
2	B-WIRE-1	32.5	22.0	101.0	A & B
	B-WIRE-2	35.5	23.0	98.5	A & B
	B-WIRE-3	36.0	23.5	102.5	A & B
6	B-SYNT-1	34.5	27.0	101.5	A & B
	B-SYNT-2	36.5	24.5	102.5	A & B
	B-SYNT-3	39.0	25.0	103.5	A & B

^a A-flexural failure by yielding tensile reinforcement, B-flexural failure by concrete crushing.

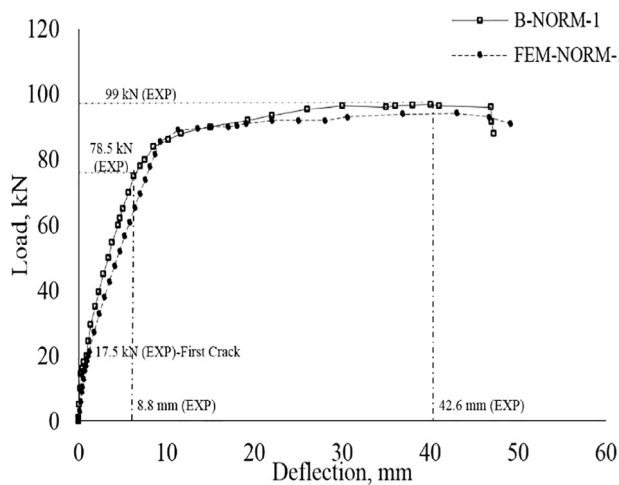


Fig. 16. Load-deflection curve of B-NOR-1.

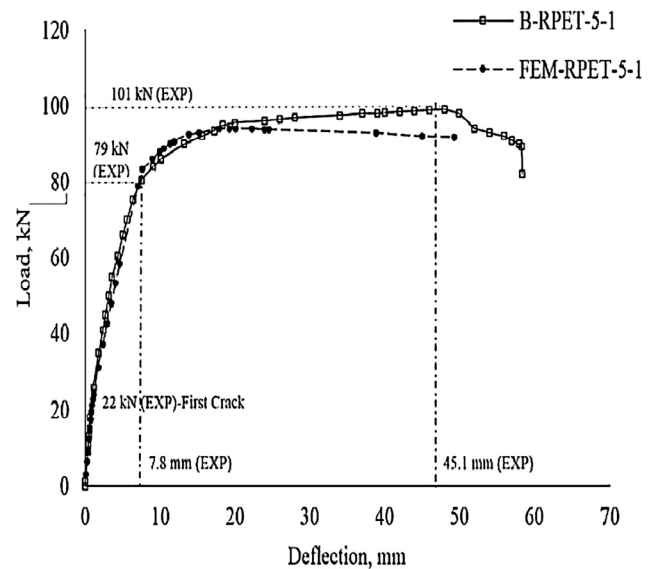


Fig. 17. Load-deflection curve of B-RPET-5-1.

ultimate load values of 99 kN, 98 kN, and 98.5 kN and exhibited flexural failure mode caused by yielding of tensile reinforcement and concrete crushing. RPET-5 beam specimens indicated that the first crack appeared at 22.0 kN, 23 kN, and 23.5 kN. RPET-5 beam specimens achieved ultimate load values of 101 kN, 98.5 kN, and 102.5 kN and exhibited flexural failure mode caused by yielding of tensile reinforcement and concrete crushing.

The flexural failure patterns of RPET-10, irregularly shaped PET, waste wire, and synthetic FC beam specimens were similar to those of RPET-5 FC beam specimens. The flexural failure modes of RPET-10, irregularly shaped PET, waste wire, and synthetic FC beam specimens were due to yielding of tensile reinforcement and concrete crushing. Normal concrete beam specimens and FC beam specimens exhibited similar failure modes. Thus, incorporating fiber into concrete was insignificant. For waste wire FC beam specimens, the first crack appeared at 23 kN, 24.5 kN, and 22.5 kN. For RPET-10 FC beam specimens, the first crack appeared at 24 kN, 23.5 kN, and 23 kN. The ultimate loads obtained by waste wire FC beam specimens were 100 kN, 98 kN, and 102.5 kN,

whereas those obtained by RPET-10 FC beam specimens were 99 kN, 98.5 kN, and 101.5 kN.

Irregularly shaped PET and synthetic FC beam specimens presented a pattern similar to those of RPET FC beams. The first crack appeared at 22.5 kN, 20.5 kN, and 21.5 kN for irregularly shaped PET FC beams and at 27 kN, 24.5 kN, and 25 kN for synthetic FC beams. The ultimate loads of irregularly shaped PET FC beams were 99.5 kN, 99 kN, and 99.5 kN, whereas those of synthetic FC beams were 104.5 kN, 101.5 kN, and 103.5 kN. Thus, the difference between the ultimate loads of normal reinforced concrete and reinforced RPET FC was insignificant. Different fiber types and fiber sizes incorporated into reinforced concrete beams presented similar results.

All sizes of the reinforced RPET FC exhibited positive results for serviceability load, with average values ranging between 28.8% and 32.3% compared to those of normal reinforced concrete beams.

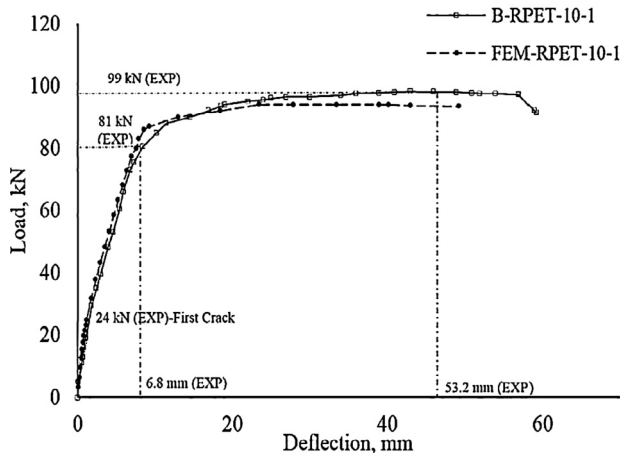


Fig. 18. Load-deflection curve of B-RPET-10-1.

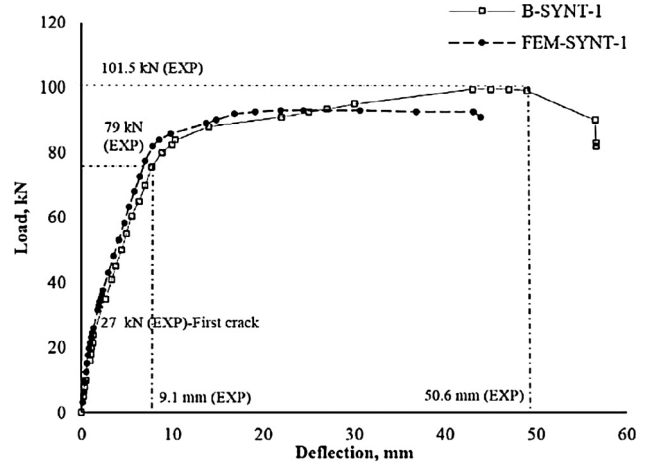


Fig. 21. Load-deflection curve of B-SYNT-1.

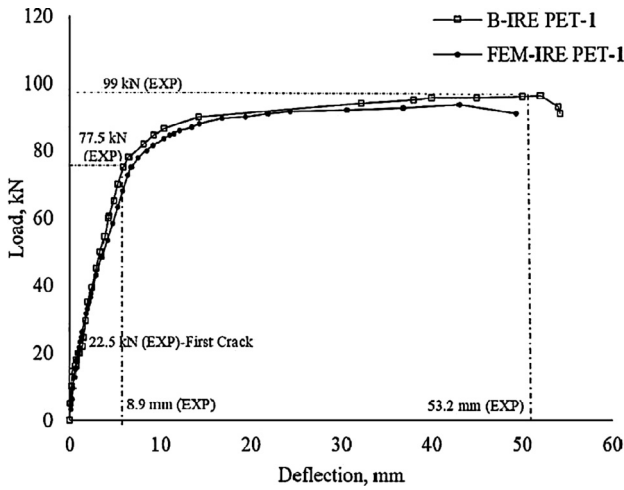


Fig. 19. Load-deflection curve of B-IRE PET-1.

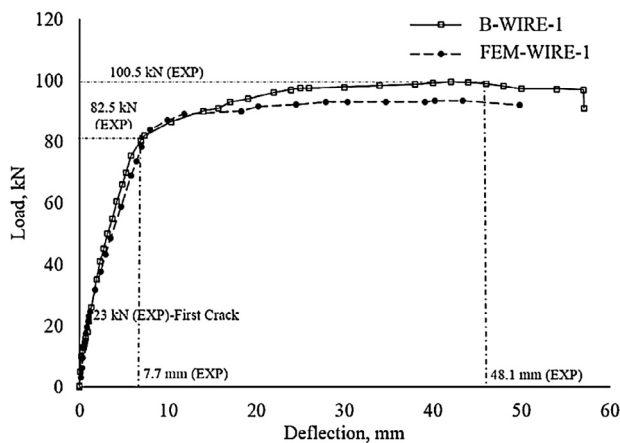


Fig. 20. Load-deflection curve of B-WIRE-1.

moderate loads. Normal concrete starts to crack after the load increases and achieves the tensile strength of concrete. The crack propagates rapidly as the load increases, and the reinforced concrete beam starts to deflect slightly. In reinforced concrete, the tensile strength of FC is higher than that of normal concrete. The moment FC starts to crack, a number of fibers continue to carry and transfer loads. Thus, structural beam integrity is maintained and beam deflection slightly increases.

Table 5 shows the summary of the loads and deflection values according to the experimental and FEM results. Based on Eurocode 2, the deflection during serviceability load is calculated as $span/250$. The span of a reinforced concrete beam is measured from one support to another support. The theoretical value calculated for deflection during serviceability load based on Eurocode 2 was 9.2 mm for a beam span of 2.5 m. The deflection during serviceability load for all reinforced concrete beam specimens was tested lower than the theoretical value, thereby achieving the requirement of less than 9.2 mm. The reinforced RPET FC beam specimens exhibited a lower value in the ratio of $\Delta_{first}/(Deflection)_{FEM}$ over the theoretical value. The results indicate that all beam specimens obtained deflection at the first crack load within the theoretical limits set by Eurocode 2. The yield load was measured by observing the load–deflection graph, wherein the yield load of the reinforced concrete beam is the load that results in yielding of tensile reinforcement [47]. The results for load and deflection during the yield stage are presented in Table 5. All beam specimens exhibited similar patterns in yield load with average values of 79 kN–81.5 kN. The pattern of the results obtained by incorporating fiber into reinforced concrete beams showed that the addition of synthetic or plastic fiber to FC beams subjected to yield load presented similar results to FC beams without added fiber. This clearly showed that synthetic or plastic FC in the beam specimen exhibited positive results under the uncracked section (linear elastic region).

The values of tensile and fracture energy which have been included in the material properties of the FEM parameters exhibited different values compared to the experimental results. However, the differences between the experimental results and the FEM results for the yield load of reinforced concrete exhibited average differences between 2.1% and 5.2%. In a preliminary study, the reinforced concrete beam specimen failed after the load dropped to approximately 15% of its maximum load. During actual testing, the load at the ultimate stage was declared when the load dropped by approximately 15% of the maximum load. Table 5 presents the experimental values for ultimate loads and their deflection at mid-span values. All beam specimens exhibited a

Reinforced synthetic fiber and irregularly shaped PET FC obtained sufficient loads of 44.4% and 21.5%, respectively, compared to normal concrete. Previous researchers claimed that adding fibers increases the serviceability load because of the effect of fiber on the tensile strength and fracture energy of FC. Therefore, the individual tensile strength of plastic fiber was retained at low to

Table 4
Load at first crack and ultimate load of normal and FC beam.

No of batch	Beam Designation	Load at first crack					Ultimate load				
		Load, (kN)	Ave. (kN)	Difference percentage compared to normal concrete, (%)	Difference percentage compared to irregular PET FC, (%)	Difference percentage compared to synthetic FC, (%)	Load, (kN)	Ave. (kN)	Difference percentage compared to normal concrete, (%)	Difference percentage compared to irregular PET FC, (%)	Difference percentage compared to synthetic FC, (%)
1	B-NOR-1	17.5		–	–17.6	–30.5	99.0	98.5	–	0.2	–4.7
	B-NOR-2	17.0	17.7				98.0				
	B-NOR-3	18.5					98.5				
2	B-RPET-5-1	22.0		28.8	6.0	–10.6	101.0	99.3	0.1	0.1	–3.8
	B-RPET-5-2	23.0	22.8				98.5				
	B-RPET-5-3	23.5					98.5				
3	B-RPET-10-1	24.0		32.3	9.3	–7.8	95.0	98.3	–0.3	0	–4.8
	B-RPET-10-2	23.5	23.5				98.5				
	B-RPET-10-3	23.0					101.5				
4	B-IRE-1	22.5		21.5	–	–15.7	99.5	98.3	–0.3	–	–4.8
	B-IRE-2	20.5	21.5				99.0				
	B-IRE-3	21.5					96.5				
5	B-WIRE-1	23.0	23.3	31.6	8.4	–8.6	101.5	98.2	–0.3	0.1	–4.8
	B-WIRE-2	24.5					94.0				
	B-WIRE-3	22.5					99.0				
6	B-SYNT-1	27.0		44.1	18.6	–	103.5	103.2	4.8	5.0	–
	B-SYNT-2	24.5	25.5				104.5				
	B-SYNT-3	25.0					101.5				

Table 5
Summary of load and deflection results.

Stage		Cracking				Yielding				Ultimate				Cracking		Yielding		Ultimate	
		Experiment		FEM		Experiment		FEM		Experiment		FEM		Ratio Exp/FEM	Ave.	Ratio Exp/FEM	Ave.	Ratio Exp/FEM	Ave.
No of batch	Beam Designation	P _{first} (kN)	Δ _{first} (mm)	P _{first} (kN)	Δ _{first} (mm)	P _{yield} (kN)	Δ _{yield} (mm)	P _{yield} (kN)	Δ _{yield} (mm)	P _{ultimate} (kN)	Δ _{ultimate} (mm)	P _{ultimate} (kN)	Δ _{ultimate} (mm)	P _{first} (kN)	Ave.	P _{yield} (kN)	Ave.	P _{ultimate} (kN)	Ave.
1	B-NOR-1	17.5	1.94	16.98	1.251	79.5	8.823	80.11	9.872	99.0	42.634	92.21	41.823	1.031		0.992		1.074	
	B-NOR-2	17.0	2.089	17.06	1.222	79.0	10.119	80.15	9.888	98.0	43.965	92.89	41.672	0.997	1.043	0.985	0.985	1.055	1.066
	B-NOR-3	18.5	1.847	16.78	1.206	78.5	11.562	80.12	9.901	98.5	42.739	92.23	41.552	1.102		0.979		1.068	
2	B-RPET-5-1	22.0	1.219	20.54	1.089	79.0	7.823	83.33	9.992	101.0	45.128	92.45	42.198	1.071		0.948		1.092	
	B-RPET-5-2	23.0	1.278	20.62	1.152	79.5	8.19	83.00	10.115	98.5	40.12	91.90	42.091	1.116	1.105	0.958	0.959	1.072	1.093
	B-RPET-5-3	23.5	1.191	20.84	1.123	81.5	8.125	83.88	9.867	102.5	44.779	91.99	42.118	1.128		0.972		1.114	
3	B-RPET-10-1	24	1.188	21.32	1.052	81.0	6.898	83.09	8.999	99.0	53.238	91.36	42.675	1.125		0.975		1.084	
	B-RPET-10-2	23.5	1.206	21.52	1.107	79.5	8.09	83.98	9.117	98.5	54.981	92.24	42.512	1.092	1.092	0.947	0.956	1.068	1.084
	B-RPET-10-3	23.0	1.072	21.73	1.129	79.5	8.006	83.99	9.349	101.5	55.036	92.33	42.89	1.058		0.947		1.099	
4	B-WIRE-1	23.0	1.062	21.28	1.121	82.5	7.74	82.46	10.214	100.5	51.218	92.13	43.01	1.080	1.101	1.001	0.979	1.091	1.089
	B-WIRE-2	24.5	1.238	21.12	1.126	80.5	7.921	82.00	10.326	98.0	54.898	92.12	42.551	1.160		0.982		1.064	
	B-WIRE-3	22.5	1.11	21.19	1.139	79.0	8.338	82.87	10.417	102.5	55.009	92.18	42.448	1.062		0.953		1.112	
5	B-IRE-1	22.5	2.078	20.60	1.006	77.5	8.88	82.24	9.783	99.5	53.181	92.33	42.44	1.092		0.942		1.078	
	B-IRE-2	20.5	1.272	20.50	1.002	80.5	8.862	82.78	9.796	99.0	50.237	91.89	42.112	1.000	1.045	0.972	0.952	1.077	1.079
	B-IRE-3	21.5	1.545	20.61	1.357	78.0	7.615	82.96	9.704	99.5	51.885	91.91	42.982	1.043		0.940		1.083	
6	B-SYNTH-1	25.5	1.219	21.86	1.211	79.0	9.051	82.91	10.033	101.5	58.528	92.77	44.512	1.17	1.15	0.953	0.972	1.094	1.096
	B-SYNTH-2	24.5	1.233	21.85	1.106	80.0	7.239	82.99	10.112	102.5	57.029	93.70	44.112	1.121		0.964		1.094	
	B-SYNTH-3	25.0	1.182	21.82	1.118	82.5	8.091	82.53	10.084	103.5	58.27	93.56	44.592	1.146		1.000		1.101	

similar pattern for ultimate load, with average values between 98.5 kN and 103.5 kN. The plotted load–deflection curves presented yield loads with average values between 77.5 kN and 82.5 kN for the beam specimens.

The comparison between reinforced concrete beam specimens with fibers and the control specimens showed that the ultimate load and mid-span deflection results were insignificant because the ultimate load satisfied the maximum load capacity of the reinforcement bar. Therefore, the maximum load did not fully carry the concrete beam but depended on the maximum tensile stress of the reinforcement design. However, the advantages of ductility in FC beams fully depend on the tensile strength of the fiber itself. Fibers with high tensile strength exhibit impressive ultimate load and ductility in reinforced FC beams.

At the end of the analysis, synthetic fiber achieved the highest ultimate load with an average value of 102.3 kN. This result is consistent with the findings of a previous research, and fibers with high tensile strength presented significant results because synthetic fiber has a tensile strength of 425 MPa. The high tensile strength of fiber tends to result in maximum fiber stress bridges during maximum bending.

4. Concluding remarks

The failure mode of the reinforced concrete beam specimens confirmed the theory that reinforced concrete beams should fail due to yielding of tensile reinforcement and not because of sudden fatal compression failure. These trends were observed in all reinforced concrete beam specimens. Therefore, the reinforced concrete beam specimens with fibers did not affect the control behavior of the strain profiles of the beams during the yield and ultimate load.

The experiments confirmed that adding RPET-5 or RPET-10 fibers to the reinforced concrete beams did not lower the deflection behavior of the control reinforced concrete beam specimens. During the cracking stage, concrete beams containing RPET-10 showed that the strength of the first crack improved by 32.3% compared to normal concrete beams. The results of the relative ductility (ultimate load) of the reinforced concrete beam specimens with RPET fibers were insignificant compared to those of normal reinforced concrete beams, except for the reinforced synthetic FC beams. However, adding RPET fibers to the reinforced concrete produced significant results, particularly in the linear elastic region.

Conflict of interest

There is no conflict of interest.

References

- [1] H. Zhang, Z. Wen, The consumption and recycling collection system of PET bottles: a case study of Beijing, China, *Waste Manage. (Oxford)* 34 (2013) 987–998.
- [2] R. Siddique, J. Khatib, I. Kaur, Use of recycled plastic in concrete: a review, *Waste Manage.* 28 (2007) 1835–1852.
- [3] T. Haktanir, K. Ari, F. Altun, O. Karahan, A comparative experimental investigation of concrete, reinforced-concrete and steel-fibre concrete pipes under three-edge-bearing test, *Constr. Build. Mater.* 21 (8) (2007) 1702–1708.
- [4] A.A. Ramezani-pour, M. Esmaili, S.A. Ghahari, M.H. Najafi, Laboratory study on the effect of polypropylene fiber on durability, and physical and mechanical characteristic of concrete for application in sleepers, *Constr. Build. Mater.* 44 (2013) 411–418.
- [5] D.G. Snelson, J.M. Kinuthia, Resistance of mortar containing unprocessed pulverised fuel ash (PFA) to sulphate attack, *Cem. Concr. Compos.* 32 (7) (2010) 523–531.
- [6] D.Y. Yoo, J.J. Park, S.W. Kim, Y.S. Yoo, Early age setting, shrinkage and tensile characteristics of ultra high-performance fiber reinforced concrete, *Constr. Build. Mater.* 41 (2013) 427–438.
- [7] D.Y. Yoo, K.H. Min, J.H. Lee, Y.S. Yoon, Shrinkage and cracking of restrained ultrahigh-performance fiber-reinforced concrete slabs at early age, *Constr. Build. Mater.* 73 (2014) 357–365.
- [8] S.S. Park, Unconfined compressive strength and ductility of fiber-reinforced cemented sand, *Constr. Build. Mater.* 25 (2) (2011) 1134–1138.
- [9] D. Foti, Preliminary analysis of concrete reinforced with waste bottles PET fibers, *Constr. Build. Mater.* 25 (2011) 1906–1915.
- [10] E.R. Silva, J.F.J. Coelho, J.C. Bordado, Strength improvement of mortar composites reinforced with newly hybrid-blended fibers: Influence of fibers geometry and morphology, *Constr. Build. Mater.* 40 (2013) 473–480.
- [11] P. Sukontasukkul, P. Pongsopha, P. Chindaprasit, S. Songpiriyakij, Flexural performance and toughness of hybrid steel and polypropylene fibre reinforced geopolymer, *Constr. Build. Mater.* 161 (2018) 37–44.
- [12] Y. Wan, J. Takahashi, Tensile and compressive properties of chopped carbon fiber tapes reinforced thermoplastics with different fiber lengths and molding pressures, *Compos. Part A* 87 (2016) 271–281.
- [13] D. Foti, S. Vacca, Comportamiento mecánico de columnas de hormigón armado reforzadas con mortero reoplástico/Mechanical behavior of concrete columns reinforced with rheoplastic mortar, *Materiales De Construcción* 63 (310) (2013) 267–282.
- [14] A. Beglarigale, H. Yazici, Pull-out behavior of steel fiber embedded in flowable RPC and ordinary mortar, *Constr. Build. Mater.* 75 (2015) 255–265.
- [15] T.A. Soylev, T. Ozturan, Durability, physical and mechanical properties of fiber reinforced concretes at low-volume fraction, *Constr. Build. Mater.* 73 (2014) 67–75.
- [16] A.E. Richardson, S. Landless, Synthetic fibres and steel fibres in concrete with regard to bond strength and toughness, *Built Environ. Res.* 2 (2) (2009) 128–140.
- [17] A.J. Babafemi, W.P. Boshoff, Tensile creep of macro-synthetic fibre reinforced concrete (MSFRC) under uni-axial tensile loading, *Cem. Concr. Compos.* 55 (2015) 62–69.
- [18] M.G. Alberti, A. Enfadaque, J.C. Galvez, on the mechanical properties and fracture behavior of polyolefin fiber-reinforced self-compacting concrete, *Constr. Build. Mater.* 55 (2014) 274–288.
- [19] T. Ochi, S. Okubo, K. Fukui, Development of recycled PET fiber and its application as concrete-reinforcing fiber, *Cem. Concr. Compos.* 29 (2007) 448–455.
- [20] B. Yesilata, Y. Isiker, P. Turgut, Thermal insulation enhancement in concretes by adding waste PET and rubber pieces, *Constr. Build. Mater.* 23 (2009) 1878–1882.
- [21] V. Vairagade, K. Kene, N. Deshpande, Investigation on compressive and tensile behavior of fibrillated, *Eng. Res. Appl.* 2 (3) (2013) 1111–1115.
- [22] J.M. Irwan, S.K. Faisal, N. Othman, H.B. Koh, A.K. Aeslina, A. Mazni, R.M. Asyraf, M.M.K. Annas, Relationship between compressive, splitting tensile and flexural strength of concrete containing granulated waste polyethylene terephthalate (PET) bottles as fine aggregate, *Adv. Mater. Res.* 795 (2013) 356–359.
- [23] L.A.P.D. Oliveira, J.P.C. Gomes, Physical and mechanical behaviour of recycled PET fibre reinforced mortar, *Constr. Build. Mater.* 25 (2011) 1712–1717.
- [24] K. Ramadevi, R. Manju, Experimental investigation on the properties of concrete with plastic PET (bottle) fibre as fine aggregates, *Int. J. Emerg. Technol. Adv. Eng.* 2 (6) (2012) 42–46.
- [25] A.M. Alani, D. Beckett, Mechanical properties of a large scale synthetic fibre reinforced concrete ground slab, *Constr. Build. Mater.* 41 (2013) 335–344.
- [26] J.P. Won, C.I. Jang, S.W. Lee, S.J. Lee, H.Y. Kim, Long-term performance of recycled PET fibre-reinforced cement composites, *Constr. Build. Mater.* 24 (5) (2010) 660–665.
- [27] F. Mahdi, H. Abbas, A.A. Khan, Strength characteristics of polymer mortar and concrete using different compositions of resins derived from post-consumer PET bottles, *Constr. Build. Mater.* 24 (2010) 25–36.
- [28] M. Nili, V. Afraouhsabet, The effects of silica fume and polypropylene fibers on the impact resistance and mechanical properties of concrete, *Constr. Build. Mater.* 24 (2010) 927–933.
- [29] A.A. Nia, M. Hedayantian, M. Nili, V.A. Sabet, An experimental and numerical study on how steel and polypropylene fibers affect the impact resistance in fibre-reinforced concrete, *Int. J. Impact Eng.* 46 (2012) 62–73.
- [30] Y. Mohammadi, S.P. Singh, S.K. Kaushik, Properties of steel fibrous concrete containing mixed fibres in fresh and hardened state, *Constr. Build. Mater.* 22 (2008) 956–965.
- [31] D. Foti, F. Paparella, Impact behavior of structural elements in concrete reinforced with PET grids, *Mech. Res. Commun.* 57 (2014) 57–66.
- [32] F. Pelisser, O.R.K. Montedo, Mechanical properties of recycled PET fibre in concrete, *Mater. Res.* 15 (4) (2012) 679–685.
- [33] S.M. Meddah, M. Bencheikh, Properties of concrete reinforced with different kinds of industrial waste fibre materials, *Constr. Build. Mater.* 23 (2009) 3196–3205.
- [34] H. Mazaheripour, S. Ghanbarpour, S.H. Mirmoradi, I. Hosseinpour, The effect of polypropylene fibers on the properties of fresh and hardened lightweight self-compacting concrete, *Constr. Build. Mater.* 25 (3) (2011) 351–358.
- [35] D. Foti, A. Romanazzi, Experimental analysis of fiber-reinforced mortar for walls in rectified brick blocks/Analisi sperimentale di malte fibrorinforzate per pareti in blocchi di laterizio rettificati, *Ceramurgia + Ceramica Acta* 41 (2) (2011) 109–118.
- [36] M. Hasan, M. Afroz, H. Mahmud, An experimental investigation on mechanical behavior of macro synthetic fibre reinforced concrete, *Int. J. Civil Environ. Eng. IJCEE-IJENS* 11 (3) (2011) 18–23.

- [37] S.B. Kim, Material and structural performance evaluation of recycled PET fiber reinforced concrete, *Cem. Concr. Compos.* 32 (2010) 232–240.
- [38] D. Foti, Innovative techniques for concrete reinforcement with polymers, *Constr. Build. Mater.* 112 (2016) 202–209.
- [39] P. Kannam, V.R. Sarella, A study on validation of shear behaviour of steel fibrous SCC based on numerical modelling (ATENA), *J. Build. Eng.* 19 (2018) 69–79.
- [40] M. Hsie, C. Tu, P.S. Song, Mechanical properties of polypropylene hybrid fiber reinforced concrete, *Mater. Sci. Eng.* 494 (1-2) (2008) 153–157.
- [41] G. Campione, Influence of FRP wrapping techniques on the compressive behavior of concrete prisms, *Cem. Concr. Compos.* 28 (5) (2006) 497–505.
- [42] F. Fraternali, V. Ciancia, R. Chechile, G. Rizzano, L. Feo, L. Incarnato, Experimental study of the thermo-mechanical properties of recycled PET fiber-reinforced concrete, *Compos. Struct.* 93 (9) (2011) 2368–2374.
- [43] J.M. Irwan, N. Othman, H.B. Koh, R.M. Asyraf, S.K. Faisal, M.M.K. Annas, The mechanical properties of PET fiber reinforced concrete from recycled bottle wastes, *Adv. Mater. Res.* 795 (2013) 347–351.
- [44] A. Peyvandi, P. Soroushian, S. Jahangirnejad, Enhancement of the structural efficiency and performance of concrete pipes through fiber reinforcement, *Constr. Build. Mater.* 45 (2013) 36–44.
- [45] H. Sammer, H. William, Z. Brian, Effect of matrix strength on pullout behavior of steel fiber reinforced very-high strength concrete composites, *Constr. Build. Mater.* 25 (1) (2010) 39–46.
- [46] M.N. Soutsos, T.T. Le, A.P. Lampropoulos, Flexural performance of fibre reinforced concrete made with steel and synthetic fibres, *Constr. Build. Mater.* 36 (2012) 704–710.
- [47] J.M. Irwan, R.M. Asyraf, N. Othman, H.B. Koh, A.K. Aeslina, M.M.K. Annas, S.K. Faisal, Deflection behaviour of irregular-shaped Polyethylene Terephthalate fibre reinforced concrete beam, *Appl. Mech. Mater.* 911 (2014) 438–442.